nature physics

Letter

https://doi.org/10.1038/s41567-022-01887-3

Probing the onset of quantum avalanches in a many-body localized system

Received: 23 December 2021

Accepted: 22 November 2022

Published online: 26 January 2023



Check for updates

Julian Léonard^{1,5,6}, Sooshin Kim ^{1,6}, Matthew Rispoli, Alexander Lukin, Robert Schittko¹, Joyce Kwan¹, Eugene Demler², Dries Sels © ^{3,4} & Markus Greiner¹⊠

Strongly correlated systems can exhibit unexpected phenomena when brought in a state far from equilibrium. An example is many-body localization, which prevents generic interacting systems from reaching thermal equilibrium even at long times^{1,2}. The stability of the many-body localized phase has been predicted to be hindered by the presence of small thermal inclusions that act as a bath, leading to the delocalization of the entire system through an avalanche propagation mechanism³⁻⁸. Here we study the dynamics of a thermal inclusion of variable size when it is coupled to a many-body localized system. We find evidence for accelerated transport of thermal inclusion into the localized region. We monitor how the avalanche spreads through the localized system and thermalizes it site by site by measuring the site-resolved entropy over time. Furthermore, we isolate the strongly correlated bath-induced dynamics with multipoint correlations between the bath and the system. Our results have implications on the robustness of many-body localized systems and their critical behaviour.

One of the founding principles of statistical physics is that a generic macroscopic system can equilibrate on its own. This means that local fluctuations in energy, magnetization or particle density can relax towards thermal equilibrium because interactions allow different parts of the system to serve as reservoirs to each other. This universal picture has been challenged by the idea of many-body localization (MBL), which suggests that systems with strong disorder can evade thermalization even in the presence of interactions^{1,2,9-15}. In one-dimensional systems, a stable MBL phase can be argued as follows: matrix elements of local operators decay exponentially with separation between two points, whereas the density of states increases exponentially with the system size. For strong disorder, matrix elements can, thus, be argued to decay faster than the density of states increases, ultimately inhibiting relaxation.

However, the existence of MBL remains a subject of debate, since it is unclear when those conditions are fulfilled¹⁶⁻²⁴. For instance, by introducing a small region with weak disorder, part of the system may be delocalized and thus give rise to local operators with non-exponential decay^{25-33,33-36}. Those local weakly disordered regions occur naturally in randomly disordered systems, when potential offsets on consecutive lattice sites accidentally coincide^{25,28,29,37,38}. The dynamics in MBL systems in the presence of a thermal region have been predicted to occur in so-called quantum avalanches, which imply that these regions grow by absorbing nearby disordered regions³⁻⁷. Under which conditions quantum avalanches can arise, run out of steam or propagate without halt determines the fate of MBL at long evolution times. Their understanding is, thus, closely connected to discerning thermalization in interacting many-body systems.

Perturbative bath-induced relaxation can often be captured in the context of Fermi's golden rule (Fig. 1a, left). In this picture, the relaxation rate $\Gamma_i = g_i^2 \rho_{\text{bath}}$ at a distance of *i* sites away from the bath is given by the product of the bath's constant density of states ρ_{bath} and coupling

Department of Physics, Harvard University, Cambridge, MA, USA. Institute for Theoretical Physics, ETH Zurich, Zurich, Switzerland. Center for Computational Quantum Physics, Flatiron Institute, New York, NY, USA. 4Department of Physics, New York University, New York, NY, USA. 5Present address: Vienna Center for Quantum Science and Technology, Atominstitut, TU Wien, Vienna, Austria. 6These authors contributed equally: Julian Léonard, Sooshin Kim. e-mail: greiner@physics.harvard.edu

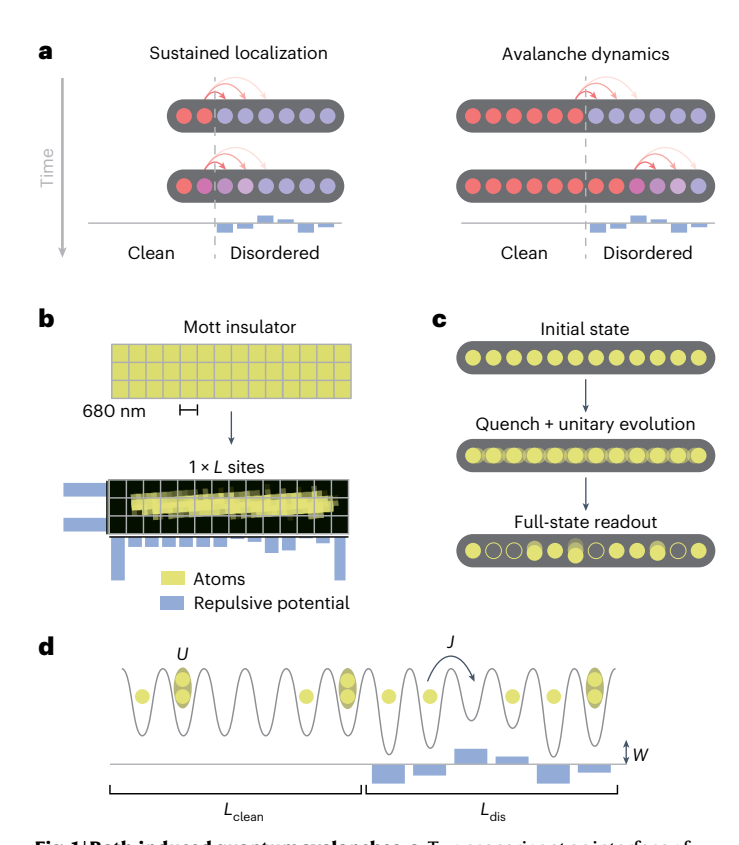


Fig. 1| **Bath-induced quantum avalanches. a**, Two scenarios at an interface of a thermal bath (clean) and a localized (disordered) region: the bath penetrates logarithmically slow and localization remains robust (left), or an avalanche thermalizes the disordered region site by site (right). **b**, Fluorescence pictures of a two-dimensional Mott insulator at unity filling, and of the initialized one-dimensional system of L sites. Projected optical potentials isolate the system and apply site-resolved offsets onto the disordered region (blue). **c**, Protocol: the initial state is brought far from equilibrium through a quantum quench by abruptly enabling tunnelling along all the neighbouring links and then evolve under the Hamiltonian, until we detect the site-resolved atom number with a fluorescence picture. **d**, System dynamics are governed by the Bose–Hubbard model with tunnelling energy J and on-site interaction energy U, extended by a disorder potential with amplitude W in the disordered region.

rate $g_i \propto J \mathrm{e}^{-\mathrm{i}/\xi_{\mathrm{loc}}}$, where ξ_{loc} is the localization length of the MBL system and J is the tunnelling rate between neighbouring sites. Consequently, within a perturbative description, MBL remains robust against a local bath, with a bath penetration into the MBL region that increases logarithmically in time.

Quantum avalanches, in contrast, are predicted to emerge from dynamics beyond this simple picture (Fig. 1a, right). A more accurate description ought to take into account that the density of states of the bath grows when the first disordered site thermalizes and hence merges with the bath. This feedback effect enhances the relaxation rate Γ_i for the next localized sites, giving rise to accelerated bath penetration into the disordered region faster than logarithmically in time. Eventually, these non-perturbative relaxation processes may lead to a full delocalization of the system if the density of states grows faster than the decay in the coupling rates.

Studying quantum avalanches within disordered systems remains a challenge due to both statistical rareness of a sufficiently large thermal inclusion and the large timescales over which the inclusion spreads through the system. Consequently, theoretical approaches often consider disordered systems that are locally coupled to a thermal bath that represents the rare region⁵. Within this canonical setting,

several signatures have been proposed to identify quantum avalanches through their short-term dynamics, including speedup compared with logarithmic spreading⁷, and back-action on the bath³. However, high demands in local control have so far hindered their experimental observation.

In this work, we explore the dynamics of an MBL system coupled to a thermal inclusion (Fig. 1) and observe phenomena that suggest the presence of non-perturbative avalanche processes. Our experimental protocol starts by preparing a Mott-insulating state with one $^{\rm 87}Rb$ atom on each site of a two-dimensional optical lattice (Fig. 1b). The system is placed in the focus of a high-resolution imaging system through which we project site-resolved repulsive potentials on individual lattice sites. We isolate a one-dimensional system of L lattice sites from the Mott insulator and add potential offsets to the lattice sites. At this point, the system remains in the product state of one atom per lattice site. We then perform a quantum quench by abruptly reducing the lattice depth (Fig. 1c). The subsequent non-equilibrium dynamics are described by the Bose–Hubbard Hamiltonian:

$$\begin{split} \hat{\mathcal{H}} &= -J\sum_{i}\left(\hat{a}_{i}^{\dagger}\hat{a}_{i+1} + \text{h.c.}\right) \\ &+ \frac{U}{2}\sum_{i}\hat{n}_{i}\left(\hat{n}_{i} - 1\right) + W\sum_{i \in L_{\text{dis}}}h_{i}\hat{n}_{i}, \end{split}$$

where $\hat{a}_{i}^{\dagger}(\hat{a}_{i})$ is the creation (annihilation) operator for a boson on site i and $\hat{n}_i = \hat{a}_i^{\dagger} \hat{a}_i$ is the particle number operator. The first term describes the tunnelling between all the neighbouring lattice sites, and the second term represents the on-site repulsive interactions. The last term introduces a site-resolved energy offset. We set $h_i = 0$ for all the lattice sites in the clean region of size $L_{\rm clean}$, whereas the energy offsets in the disordered region of size $L_{\rm dis}$ follow a quasi-periodic disorder distribution $h_i = \cos(2\pi\beta i + \phi)$ for $1/\beta \approx 1.618$, phase ϕ and amplitude W. The quasi-periodic distribution avoids nearby lattice sites to coincidentally have similar energy offsets, which inhibits the presence of secondary rare regions within the disordered region³⁹. After a variable evolution time, we read out the site-resolved atom number by fluorescence imaging. The applied unitary evolution preserves the initial purity of 99.1(2)% per site^{13,40}. All the observables are averaged over 200 disorder realizations with different ϕ values. The tunnelling time $\tau = \hbar/J = 4.3(1)$ ms (with the reduced Planck constant \hbar), the interaction strength U = 2.87(3) J and the number of disordered sites $L_{dis} = 6$ remain constant in all the experiments.

We first use the full site-resolved readout of our microscope to investigate the local transport dynamics in the system. The connected density-density correlations $\langle \hat{n}_i \hat{n}_j \rangle_c = \langle \hat{n}_i \hat{n}_j \rangle - \langle \hat{n}_i \rangle \langle \hat{n}_j \rangle$ detect correlations between the particle numbers on sites i and j (ref. 15). Negative values of $\langle \hat{n}_i \hat{n}_i \rangle$ signal anti-correlated density fluctuations and thus particle motion between the involved sites (Fig. 2a). In the following, we consider a system with $L_{clean} = 6$ at disorder strength W = 9.1J for different evolution times Tafter the quantum quench. At the beginning of evolution $(T = 0\tau)$, we do not detect any correlations, because the initial state is a product state. After short evolution times $(T \lesssim \tau L)$, we observe the buildup of spatially dependent anti-correlations in the system. Within the clean region, all the lattice sites develop mutual anti-correlations, signalling delocalized particles. In contrast, the anti-correlations in the disordered region remain short ranged, indicating localized particles. Overall, these properties persist up to long evolution times $(T \gg \tau L)$. To quantify the emergence of a bath, we extract the mean and variation of the off-diagonal correlations in the clean region (Fig. 2b). We find that within a few tunnelling times, the clean region reaches its steady state with similar correlations across all the pairs of sites, indicating that it starts to act as a thermal bath to the disordered region.

For long evolution times $(T \gg \tau L)$, we additionally observe the buildup of anti-correlations between the lattice sites in the clean and

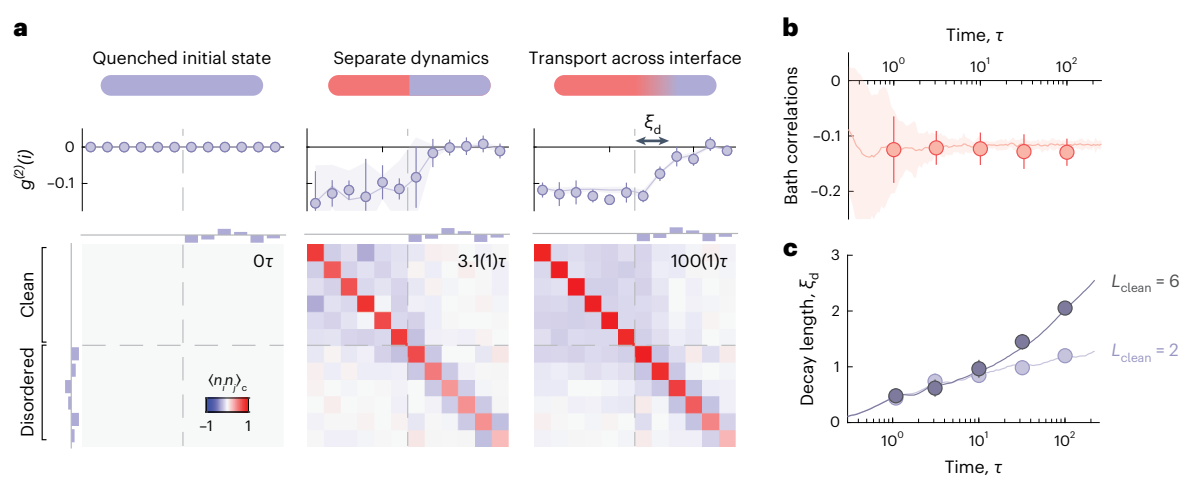


Fig. 2 | **Accelerated transport across the clean-disorder interface. a**, Density correlations for all the pairs of sites in a system consisting of $L_{\rm clean} = L_{\rm dis} = 6$ at disorder strength W = 9.1). After a quantum quench, an uncorrelated initial state (left) develops separate dynamics within each subsystem (centre), followed by slow particle transport across the clean-disorder interface (grey dashed lines) for evolution times much greater than $L_{\rm clean}$ and $L_{\rm dis}$ (right). The cuts show the total density correlations $g^{(2)}(i)$ of the clean region with site i (that is, the average of top six rows, excluding the diagonal), featuring homogeneous coupling among the clean sites, and approximately exponentially decaying anti-correlations with the distance of the disordered site from the interface. The error bars denote the

standard deviation among the different entries. \mathbf{b} , Correlations within the clean region reach a steady state within few tunnelling times, indicating the emergence of a bath. The error bars denote the standard deviation among the different entries. \mathbf{c} , Decay length ξ_a of the total density correlations accelerates at long evolution times. For a smaller clean region of $L_{\text{clean}}=2$, contrarily, the correlations continue to grow logarithmically. The error bars denote the standard error of the mean. The solid lines in all the panels show the prediction from exact numerics without free parameters, with shaded areas in \mathbf{a} and \mathbf{b} denoting the standard deviation among the different entries. The error bars are below the marker size, if not visible.

disordered regions, which is evidence for transport dynamics across the interface (Fig. 2a, right). Each disordered site is similarly anti-correlated to all the clean sites, which confirms that the clean region acts as a heat bath for the disordered region. Motivated by this picture, we extract the mean correlations of the clean region $g^{(2)}(i) = \overline{\langle \hat{n}_i \hat{n}_j \rangle_c}|_{j \in L_{\text{clean}}}$ by averaging the correlations of each site i with all clean sites j (Fig. 2a, cuts). The results are consistent with an exponential decay with distance from the clean region, in agreement with the Fermi's golden rule picture of exponentially decaying couplings between the bath and MBL.

Although a static bath spectrum causes bath correlations to penetrate the MBL logarithmically in time, a signature of quantum avalanche is an accelerated increase, faster than logarithmically in time. To test this picture, we quantify the correlation decay into the disordered region by measuring the average distance $\xi_{\rm d} = -\sum_{i\in L_{\rm dis}} i \times g^{(2)}(i)$ from the clean region over which anti-correlations form (Fig. 2c). At short times, the decay length $\xi_{\rm d}$ increases logarithmically in time, but accelerates at long evolution times. We contrast this observation with a system having $L_{\rm clean}$ = 2, where we do not find any accelerating transport dynamics.

We next examine the local thermalization dynamics across the system. The microscopic readout enables us to measure the full atom number distribution on each site (Fig. 3a). Lattice sites in the clean region show a distribution corresponding to a thermal ensemble, whereas lattice sites in the disordered region show a distribution with enhanced probability for one particle, the initial state of the system. We quantify the site-resolved thermalization dynamics with the entropy per particle $s_i = -\sum_{n_i} p(n_i) \log p(n_i)/\langle \hat{n}_i \rangle$ on site i from the atom number distributions. We observe reduced thermalization dynamics of the disordered sites with increasing distance from the interface (Fig. 3b,c). Moreover, the data suggest that the dynamics are first stationary until thermalization sets in with a delay that increases with the site's distance from the interface. This picture is confirmed by our exact numerical calculations.

The accelerated transport indicates that the long-term dynamics are driven by processes that go beyond a perturbative coupling to the

bath. We investigate this effect through multipoint correlations^{15,41}. The presence of non-zero three-point connected correlations $\langle \hat{n}_i \hat{n}_i \hat{n}_k \rangle$ signals the presence of entanglement among all the involved lattice sites, which cannot be explained in a perturbative, semiclassical description. We evaluate the connected correlations $g^{(3)}(i,j) = \overline{\langle \hat{n}_i \hat{n}_j \hat{n}_k \rangle_c}|_{k \in L_{\text{clean}}}$ among two disordered sites i and j and clean site k, averaged over all possible k values (Fig. 4a). We find a strong dependence on the involved disordered sites: correlations are strong close to the interface, whereas they become weaker for distant sites. We quantify this behaviour by considering the correlations as a function of the mean distance $\bar{d} = (i + i)/2$ of the two disordered sites from the clean region (Fig. 4b). Indeed, the correlations decrease with increasing distance from the clean region, comparable to decay length $\xi_{\rm d}$. This demonstrates that the accelerated transport is driven by many-body processes, a key property for quantum avalanches. We quantify the presence of many-body correlations at different disorder strengths by taking their average as $\overline{g^{(3)}}(i,j)|_{i,j\in L_{\mathrm{dis}}}$ (Fig. 4c,d). The correlations are present throughout the covered disorder range with a maximum at intermediate strengths, close to the estimated critical point of the system¹⁵.

In conclusion, we experimentally realized a clean-disordered interface and studied the emerging thermalization dynamics. We observed an accelerated intrusion of the bath in the MBL system, its evolution into thermal equilibrium site after site and the many-body correlations between the two subsystems—the hallmarks of quantum avalanches. In future, our experiments can be readily extended in many ways. For example, by increasing the system size of the disordered region, one could explore the interplay at intermediate disorder strengths in a quantitative way through its scaling behaviour, that is, by increasing the system size at constant ratio of L_{clean} and L_{dis} , which may provide insights into the critical behaviour of the transition. An interesting extension would also be the influence of the statistical distribution of the disorder on the critical behaviour of the system. Furthermore, engineering other heterostructures with quantum gas microscopes may provide an avenue to study phenomena in the physics of interfaces or to build atomtronic devices.

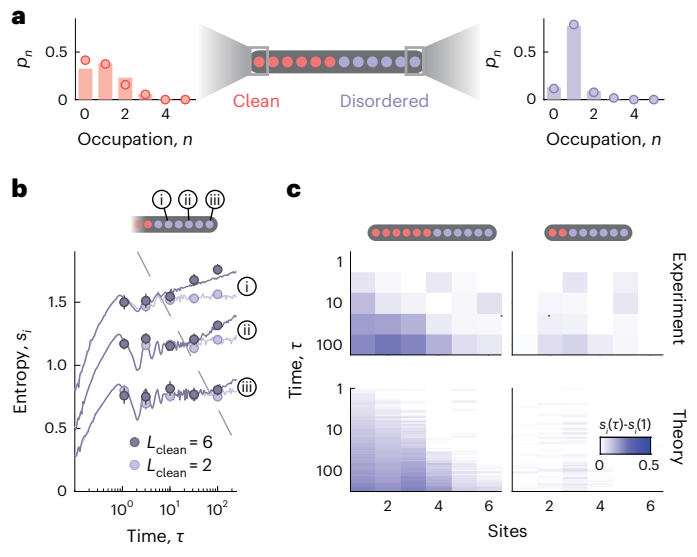


Fig. 3 | **Site-resolved thermalization dynamics. a**, Atom-number probability distribution for the edge sites in the clean region (left) and the disordered region (right), measured after 100τ in a system consisting of $L_{\rm clean} = L_{\rm dis} = 6$ at disorder strength W = 9.1/. **b**, Local entropy per particle $s_i = -\sum_n p_n \log p_n / \langle \hat{n}_i \rangle$ for selected disordered sites, extracted from the atom number distribution on each site i. The entropy grows after a stationary evolution whose length increases with distance from the interface (dashed grey line). For a smaller clean region of $L_{\rm clean} = 2$, in contrast, the growth is absent. Traces are vertically offset for better visibility. **c**, Local entropy s_i , offset by $s_i(1\tau)$ for all the disordered sites. The solid lines (bars in **a**) show the prediction from exact numerics without free parameters. The error bars denote the standard error of the mean (below the marker size in **a**).

Online content

Any methods, additional references, Nature Portfolio reporting summaries, source data, extended data, supplementary information, acknowledgements, peer review information; details of author contributions and competing interests; and statements of data and code availability are available at https://doi.org/10.1038/s41567-022-01887-3.

References

- Alet, F. & Laflorencie, N. Many-body localization: an introduction and selected topics. C. R. Phys. 19, 498–525 (2018).
- Abanin, D. A., Altman, E., Bloch, I. & Serbyn, M. Colloquium: many-body localization, thermalization, and entanglement. Rev. Mod. Phys. 91, 021001 (2019).
- Nandkishore, R. & Gopalakrishnan, S. Many body localized systems weakly coupled to baths. *Ann. Phys.* 529, 1600181 (2017).
- De Roeck, W. & Huveneers, F. Stability and instability towards delocalization in many-body localization systems. *Phys. Rev. B* 95, 155129 (2017).
- Luitz, D. J., Huveneers, F. & De Roeck, W. How a small quantum bath can thermalize long localized chains. *Phys. Rev. Lett.* 119, 150602 (2017).
- Thiery, T., Huveneers, F., Müller, M. & De Roeck, W. Many-body delocalization as a quantum avalanche. *Phys. Rev. Lett.* 121, 140601 (2018).
- Crowley, P. J. D. & Chandran, A. Avalanche induced coexisting localized and thermal regions in disordered chains. *Phys. Rev. Research* 2, 033262 (2020).
- Morningstar, A., Colmenarez, L., Khemani, V., Luitz,
 D. J. & Huse, D. A. Avalanches and many-body resonances in many-body localized systems. *Phys. Rev. B* **105**, 174205 (2022).

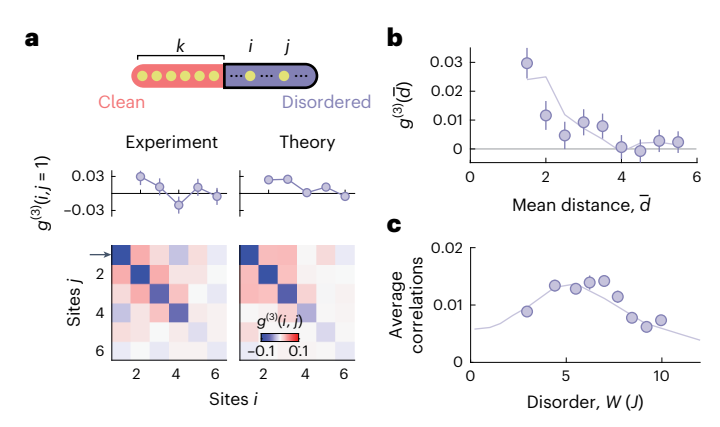


Fig. 4 | **Bath-induced many-body correlations. a**, Three-point correlations $\langle \hat{n}_i \hat{n}_j \hat{n}_k \rangle_c$ among pairs of disordered sites i and j and one clean site k (averaged over all the clean sites k) in a system with $L_{\text{clean}} = L_{\text{dis}} = 6$ at disorder strength W = 9.1/ and evolution time $100(1)\tau$. The presence of multipoint correlations demonstrates non-perturbative dynamics: delocalization is driven through many-body processes between the disordered region and clean region. **b**, Averaging over entries with equal mean distance $\overline{d} = (i+j)/2$ from the clean region shows a decay of correlations with the distance from the bath over several lattice sites, comparable to decay length ξ_d , **c**, Average over all the off-diagonal entries displays a maximum for intermediate disorder for the MBL-bath entanglement. The solid lines show the prediction from exact numerics without free parameters. The error bars denote the standard error of the mean.

- Schreiber, M. et al. Observation of many-body localization of interacting fermions in a quasirandom optical lattice. *Science* 349, 842–845 (2015).
- 10. Smith, J. et al. Many-body localization in a quantum simulator with programmable random disorder. *Nat. Phys.* **12**, 907–911 (2016).
- Choi, J.-Y. et al. Exploring the many-body localization transition in two dimensions. Science 352, 1547–1552 (2016).
- 12. Rubio-Abadal, A. et al. Many-body delocalization in the presence of a quantum bath. *Phys. Rev. X* **9**, 041014 (2019).
- Lukin, A. et al. Probing entanglement in a many-body-localized system. Science 364, 256–260 (2019).
- Lüschen, H. P. et al. Observation of slow dynamics near the many-body localization transition in one-dimensional quasiperiodic systems. *Phys. Rev. Lett.* 119, 260401 (2017).
- Rispoli, M. et al. Quantum critical behaviour at the many-body localization transition. *Nature* 573, 385–389 (2019).
- Abanin, D. A. et al. Distinguishing localization from chaos: challenges in finite-size systems. Ann. Phys. 427, 168415 (2021).
- Panda, R. K., Scardicchio, A., Schulz, M., Taylor, S. R. & Žnidarič, M. Can we study the many-body localisation transition? *Europhys. Lett.* 128, 67003 (2019).
- Sierant, P., Delande, D. & Zakrzewski, J. Thouless time analysis of Anderson and many-body localization transitions. *Phys. Rev. Lett.* 124, 186601 (2020).
- Šuntajs, J., Bonča, J., Prosen, T. & Vidmar, L. Quantum chaos challenges many-body localization. *Phys. Rev. E* **102**, 062144 (2020).
- Šuntajs, J., Bonča, J., Prosen, T. & Vidmar, L. Ergodicity breaking transition in finite disordered spin chains. *Phys. Rev. B* 102, 064207 (2020).
- Luitz, D. J. & Lev, Y. B. Absence of slow particle transport in the many-body localized phase. *Phys. Rev. B* **102**, 100202 (2020).
- Kiefer-Emmanouilidis, M., Unanyan, R., Fleischhauer, M. & Sirker, J. Evidence for unbounded growth of the number entropy in many-body localized phases. *Phys. Rev. Lett.* 124, 243601 (2020).

- 23. Kiefer-Emmanouilidis, M., Unanyan, R., Fleischhauer, M. & Sirker, J. Absence of true localization in many-body localized phases. *Phys. Rev. B* **103**, 024203 (2021).
- 24. Sels, D. Bath-induced delocalization in interacting disordered spin chains. *Phys. Rev. B* **106**, L020202 (2022).
- Agarwal, K., Gopalakrishnan, S., Knap, M., Müller, M. & Demler,
 E. Anomalous diffusion and Griffiths effects near the many-body localization transition. *Phys. Rev. Lett.* 114, 160401 (2015).
- Bar Lev, Y., Cohen, G. & Reichman, D. R. Absence of diffusion in an interacting system of spinless fermions on a one-dimensional disordered lattice. *Phys. Rev. Lett.* 114, 100601 (2015).
- Žnidarič, M., Scardicchio, A. & Varma, V. K. Diffusive and subdiffusive spin transport in the ergodic phase of a many-body localizable system. *Phys. Rev. Lett.* 117, 040601 (2016).
- Gopalakrishnan, S., Agarwal, K., Demler, E. A., Huse, D. A. & Knap, M. Griffiths effects and slow dynamics in nearly many-body localized systems. *Phys. Rev. B* 93, 134206 (2016).
- Agarwal, K. et al. Rare-region effects and dynamics near the many-body localization transition. *Ann. Phys.* 529, 1600326 (2017).
- Potter, A. C., Vasseur, R. & Parameswaran, S. A. Universal properties of many-body delocalization transitions. *Phys. Rev. X* 5, 031033 (2015).
- Vosk, R., Huse, D. A. & Altman, E. Theory of the many-body localization transition in one-dimensional systems. *Phys. Rev. X* 5, 031032 (2015).
- Gopalakrishnan, S. et al. Low-frequency conductivity in many-body localized systems. Phys. Rev. B 92, 104202 (2015).
- Weiner, F., Evers, F. & Bera, S. Slow dynamics and strong finite-size effects in many-body localization with random and quasiperiodic potentials. *Phys. Rev. B* 100, 104204 (2019).
- 34. Khemani, V., Lim, S. P., Sheng, D. N. & Huse, D. A. Critical properties of the many-body localization transition. *Phys. Rev. X* **7**, 021013 (2017).

- Khemani, V., Sheng, D. N. & Huse, D. A. Two universality classes for the many-body localization transition. *Phys. Rev. Lett.* 119, 075702 (2017).
- Kelly, S. P., Nandkishore, R. & Marino, J. Exploring many-body localization in quantum systems coupled to an environment via Wegner-Wilson flows. *Nucl. Phys. B* 951, 114886 (2020).
- Griffiths, R. B. Nonanalytic behavior above the critical point in a random Ising ferromagnet. *Phys. Rev. Lett.* 23, 17–19 (1969).
- 38. McCoy, B. M. Incompleteness of the critical exponent description for ferromagnetic systems containing random impurities. *Phys. Rev. Lett.* **23**, 383–386 (1969).
- 39. Setiawan, F., Deng, D.-L. & Pixley, J. H. Transport properties across the many-body localization transition in quasiperiodic and random systems. *Phys. Rev. B* **96**, 104205 (2017).
- Kaufman, A. M. et al. Quantum thermalization through entanglement in an isolated many-body system. *Science* 353, 794–800 (2016).
- 41. Kubo, R. Generalized cumulant expansion method. *J. Phys. Soc. Jpn* **17**, 1100–1120 (1962).

Publisher's note Springer Nature remains neutral with regard to jurisdictional claims in published maps and institutional affiliations.

Springer Nature or its licensor (e.g. a society or other partner) holds exclusive rights to this article under a publishing agreement with the author(s) or other rightsholder(s); author self-archiving of the accepted manuscript version of this article is solely governed by the terms of such publishing agreement and applicable law.

© The Author(s), under exclusive licence to Springer Nature Limited 2023

Acknowledgements

We acknowledge fruitful discussions with K. Agarwal, V. Khemani, M. Knap, M. Lebrat and J. Marino. We are supported by grants from the National Science Foundation, the Gordon and Betty Moore Foundations EPiQS Initiative, an Air Force Office of Scientific Research MURI program, an Army Research Office MURI program, the Swiss National Science Foundation (J.L.) and the NSF Graduate Research Fellowship Program (S.K.). The Flatiron Institute is a division of the Simons Foundation. D.S. is supported by the AFOSR grant FA9550-21-1-0236 and NSF grant OAC-2118310.

Author contributions

J.L., S.K., M.R., A.L., R.S. and J.K. contributed to conducting the experiment, and collecting and analysing the data. S.K. performed the numerical simulations. The theoretical concepts were developed together with D.S. and E.D. M.G. supervised the work. All the authors contributed to writing the manuscript and discussions.

Competing interests

M.G. is co-founder and shareholder of QuEra Computing. All other authors declare no competing interests.

Additional information

Supplementary information The online version contains supplementary material available at https://doi.org/10.1038/s41567-022-01887-3.

Correspondence and requests for materials should be addressed to Markus Greiner.

Peer review information *Nature Physics* thanks Giovanni Modugno and the other, anonymous, reviewers for their contribution to the peer review of this work.

Reprints and permissions information is available at www.nature.com/reprints.